Medicon Agriculture & Environmental Sciences
Volume 2 Issue 1 January 2022
Research Article

The Numerical Simulation of Pollutant Transport in Shallow Water Flows

Kissami Imad[2]* and Ziggaf Moussa[1,2,3]

[1]*ENSAO, LMCS, Complexe Universitaire, B.P. 669, 60000 Oujda, Morocco*

[2]*MSDA, Mohammed VI Polytechnic University Lot 660, 43150 Ben Guerir, Morocco*

[3]*Université Sorbonne Paris Nord, LAGA, CNRS, UMR 7539, F-93430, Villetaneuse, France*

***Corresponding Author:** Kissami Imad, MSDA, Mohammed VI Polytechnic University Lot 660, 43150 Ben Guerir, Morocco.

Received: November 27, 2021; **Published:** December 30, 2021

Abstract

A real test using the finite volume method is presented for the numerical simulation of the pollutant transport by water flows. Shallow water equations, bottom friction forces, wind shear stresses, and Coriolis effect are used to model the water flow while a transport-diffusion equation is used to model the advection and dispersion of the pollutant concentration. The finite volume method used has been the subject of several works (see e.g. [3, 4, 17]) it is a simple discretization of centered type for the source terms, can handle complex topography by using non-uniform triangular grids while keeping the conservation property. The C-property based on checking the balance between the convection term and the background profile is satisfied. The monitoring of the pollutant concentration in the computational domain during its dispersion process is taken into account. The focus of this study is on an application of pollution dispersion in the Nador lagoon in Morocco. The results are presented using different tidal conditions and wind-induced flow fields in the lagoon.

Keywords: Well balanced scheme; Complex topography; Shallow water flows; Finite volume method; Pollutant transport

Introduction

In recent years, increasing pollution in rivers, lagoons, and coastal areas has focused the attention of policymakers around the world on environmental protection issues. In many situations, these pollution problems have a significant impact on the ecology and the environment and can cause a potential risk to human health and the local economy. The ecological qualities of these environments have been relatively affected in recent years by human activities, particularly pollution from sewage and waste dumped on the banks, as well as hydrocarbons from industrial ships. These pollutants, if not quickly removed, can harm humans. This manifests itself in damage to biological resources, the risk to human health, a hindrance to to maritime activities including fishing and alteration of the quality of seawater in terms of its use.

In addition, these environments have been the subject of numerous studies concerning water quality, currents, bathymetry, fauna, fishing, and aquaculture. These studies have targeted mainly the environmental aspect of the lagoon and are of a biological, sedimentological, geochemical, or economic nature, geochemical or economic. However, there are not many studies from a numerical point of view concerning the transport of pollutants in the vicinity of these locations.

In this study, the focus is on the application of the developed numerical method to the dispersion of pollution in the lagoon of Nador, located on the north-east coast of Morocco, is an ecosystem that is of great biological, ecological and economical interest. It covers an

area that exceeds 120 km 2 and a maximum depth of 8 m,, and is fed by water of the Mediterranean through a grau known as 'Bokhana', the freshwater waterways, the rejections of the untreated human activities (agriculture and urban water industry: metallurgy, textile, etc...), and by water of purification plant. This lagoon has been the subject of several scientific studies ranging from morphodynamic studies to geological research. Its strategic position makes this research indispensable to understanding the phenomena of pollutant transport and how to get rid of them. However, these studies are essential as they act as a means of prediction and allow the establishment of risk maps. By using mathematical modeling and numerical methods, it is now possible to predict changes due to pollution and thus to plan strategies and interventions for environmental protection in the case of risk to human health. Necessary interventions for the protection of the environment in the case of risk to human health and the local human health and the local economy. The introduction and use of such types of measures are, however, impossible without a good knowledge of the various processes involved, such as the formation of water flows and the formation of water flows and the transport and dispersion of pollutants.

To obtain an approximate numerical solution of the governing equations, we implement a finite volume solver recently developed in [2, 19]. The main advantages of the proposed finite volume method are the simplicity of implementation, the implementation on unstructured meshes allowing to handle the most complex shapes of the study domain, the simultaneous advection in time of the water flow and the pollutant concentration, solving both problems at the same time and with the same accuracy, the ability to handle calculations of slowly varying flows or concentrations as well as rapidly varying flows also containing shocks or discontinuities. In the calculations presented in this paper, the ability to satisfy the exact C-property and to guarantee positive values of both the water level and the pollutant concentration in transient simulations. The results presented in this paper demonstrate the high resolution of the proposed method and confirm its ability to provide accurate and efficient simulations of pollutant transport by water flows including complex topography and frictional forces on non-uniform triangular meshes.

To give an organization of the paper. In Section 2 we will present the pollutant transport model in shallow water flows. In Section 3 a detailed description of the numerical method will be given. Section 4 we will discuss our computational results with the actual transport and hydrodynamic phenomenon in the lagoon. Section 5 contains the some conclusions and remarks.

Governing equation

The mathematical model used to describe free surface flows is based on the two-dimensional shallow water equations. It is recalled that these equations, which are now fairly well known in the literature, are obtained by vertically integrating the incompressible three-dimensional Navier-Stokes equations under the assumptions of hydrostatic pressure and vertically averaged velocities [9]. The turbulence and viscosity terms are not taken into account in this study. In the case where a pollutant is discharged into the flow, the following pollutant transport and diffusion equation must be coupled to the shallow water equations. The coupled system can be written in the following form:

$$\begin{cases} \partial_t h + \nabla \cdot (h\mathbf{u}) = 0 \\ \partial_t h\mathbf{u} + \nabla \cdot (h\mathbf{u} \otimes \mathbf{u}) + \dfrac{1}{2}\boldsymbol{\nabla}(gh^2) = -gh\boldsymbol{\nabla}Z - f_c \times h\mathbf{u} - r(h,\mathbf{u}) + \tau(h\mathbf{u}) \\ \partial_t hC + \nabla \cdot (h\mathbf{u}C) - \nabla \cdot (hD\nabla C) = hQ \end{cases} \tag{1}$$

Where the unknowns are always the water height h, the horizontal speed mean $\mathbf{u} = (u,v)^T$ and the average concentration of the pollutant C. g is the acceleration of gravity, Z designates the profile of the domain bottom, $r(h,\boldsymbol{u}) = (rf_x, rf_y) = \eta^2 g h^{-1/3}|\boldsymbol{u}|\boldsymbol{u}$, are the friction terms of the water with the bottom, such as η is the Manning roughness [11]. $\tau(h,\breve{\mathbf{u}}) = (\tau_{s_x}, \tau_{s_y}) = \frac{1}{2}\breve{C}_f|\breve{\mathbf{u}}|\breve{\mathbf{u}}$, in which $\breve{\mathbf{u}} = (\breve{u},\breve{v})^T$ represents the wind speed and $\breve{C}_f$ is the coefficient of wind friction with water. $D = (D_x, D_y)^T$ is the diffusion coefficients in the two directions of space and Q represents the source of the pollutant.

It should be noted that the geometry of the water body in our computational domain reveals that the horizontal length scale is several orders of magnitude higher than the vertical length scale. Furthermore, the pollutant is assumed to be released at the free surface

and remains on the water surface during the whole simulation time. The use of the two-dimensional hydrodynamic model coupled with the advection-diffusion equation (1) is therefore well justified. In terms of the flow variables $\mathbf{W}(h,hu,hv,hC)^T$, the system (1) can be written in the following vector form:

$$\frac{\partial \mathbf{W}}{\partial t} + \nabla \cdot (\mathbb{F}(\mathbf{W}) - \tilde{\mathbb{F}}(\mathbf{W})) = S(\mathbf{W}) + R(\mathbf{W}) \tag{2}$$

Where

$$\mathbb{F}(\mathbf{W}) = \left(\begin{pmatrix} hu \\ hu^2 + \frac{1}{2}gh^2 \\ huv \\ huC \end{pmatrix}, \begin{pmatrix} hv \\ huv \\ hv^2 + \frac{1}{2}gh^2 \\ hvC \end{pmatrix} \right)^T, \quad \tilde{\mathbb{F}}(\mathbf{W}) = \left(\begin{pmatrix} 0 \\ 0 \\ 0 \\ hD_x\partial_x C \end{pmatrix}, \begin{pmatrix} 0 \\ 0 \\ 0 \\ hD_y\partial_y C \end{pmatrix} \right)^T,$$

$$S(\mathbf{W}) = \begin{pmatrix} 0 \\ -gh\partial_x Z \\ -gh\partial_y Z \\ 0 \end{pmatrix}, \quad R(\mathbf{W}) = \begin{pmatrix} 0 \\ f_c hv - r_{f_x} + \tau_{s_x} \\ -f_c hu - r_{f_x} + \tau_{s_y} \\ hQ \end{pmatrix}.$$

Numerical method

The numerical resolution of the system (2) is very difficult and is still the subject of much recent work [14, 20, 21]. Indeed, on the one hand, the non-linear character of this system combined with its hyperbolicity excludes the use of analytical techniques for most practical problems, on the other hand, one can end up with discontinuous solutions that can be obtained even if the initial data is regular. On the other hand, the presence of steep source terms resulting from the irregularity of the bottom of the domain can make most of the existing classical schemes inappropriate. Moreover, many articles have been devoted in the last years to the construction of schemes verifying the so-called equilibrium or lake or rest property for free-surface flows with variable topography (see, e.g. [1], [7] and [12]). Therefore, it is necessary to design and develop an accurate and efficient numerical algorithm to solve this type of equation.

Spatial discretization

In this section, we will discuss the numerical computation of spatial derivatives. Therefore we propose to apply the SRNH finite volume solver described in the work of F. Benkhaldoun et al. (see, e.g. [5, 18]) in order to take into account the pollutant transport-diffusion equation in the model. The modification carried out on the discretization of the source terms describing the bottom variation will make it possible to obtain an equilibrium scheme while keeping the accuracy in space. It is recalled that the construction of the numerical scheme is based on the hyperbolicity of the system and on the self-similarity of the solution.

Finite volume discretization

The finite volume formulation starts with the discretization of the computational domain by a finite set of control volumes. We consider the "cell-centered" finite volume formulation (see Figure 1). By integrating (2) over a control volume T_i and using Green's divergence formula, we obtain the following integral system:

$$\frac{\partial}{\partial t}\int_\Omega W dV + \oint_{\partial\Omega} \mathbb{F}(W)\cdot \mathbf{n} d\sigma = \int_\Omega (S(W) + R(W)) dV, \tag{3}$$

Where Ω is the domain of interest, $\partial\Omega$ is the boundary surrounding, $\mathbf{n}$ is the normal vector to $\partial\Omega$ in the outward direction, dV and $d\sigma$ are respectively the surface element and the length element. The problem domain is first discretized into a set of triangular cells forming an unstructured computational mesh.

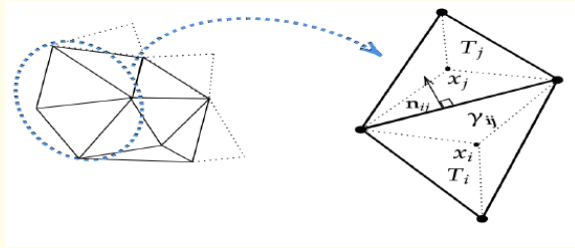

Figure 1: Generic definition of the Ω domain and the control cells of the mesh.

We use the following notations:

- x_i, centroid of the cell T_i,
- γ_{ij}, boundary edge between the cells T_i and T_j,
- $|\gamma_{ij}|$, length of γ_{ij},
- $|T_i|$, area of the cell T_i,
- $\boldsymbol{n}_{ij}$, unit normal to γ_{ij}, outward to T_i such as, $\boldsymbol{n}_{ji} = -\boldsymbol{n}_{ij}$.

The SRNH scheme is formulated by considering only the convective part of the system (2) and the source term describing the bottom of the domain:

$$\frac{\partial \mathbf{W}}{\partial t} + \nabla \cdot \mathbb{F}(\mathbf{W}) = S(\mathbf{W}) \tag{4}$$

This scheme consists of two steps: a predictor step and a corrector step. The algorithm starts with a projection of the system (4) on the nominal η and the tangential τ to obtain.

$$\frac{\partial \mathbf{U}}{\partial t} + \nabla \cdot \mathbf{F}_\eta(\mathbf{U}) = 0 \tag{5}$$

Where

$$\mathbf{U} = \begin{pmatrix} h \\ hu_\eta \\ hu_\tau \\ hC \\ Z \end{pmatrix} \quad \text{and} \quad \mathbf{F}_\eta(\mathbf{U}) = \begin{pmatrix} hu_\eta \\ hu_\eta + \frac{1}{2}gh^2 + gh\partial_\eta Z \\ hu_\eta u_\tau \\ hCu_\eta \\ 0 \end{pmatrix}$$

$u_\eta := \boldsymbol{u} \cdot \boldsymbol{n} = u \cdot n_x + v \cdot n_y$ and $u_\tau := v \cdot n_x - u \cdot n_y$ are the normal and tangential velocities respectively. The predictor step is therefore formulated for this projected system as follows:

$$\mathbf{U}_{ij}^n = \frac{1}{2}(\mathbf{U}_i^n + \mathbf{U}_j^n) - \frac{1}{2} sgn[\nabla \mathbf{F}_\eta(\bar{\mathbf{U}}_{ij}^n)](\mathbf{U}_j^n - \mathbf{U}_i^n) \tag{6}$$

Such that, we note $sgn[\nabla \mathbf{F}_\eta]$ is the sign of a matrix $\nabla \mathbf{F}_\eta$. and $\bar{\mathbf{U}}_{ij}^n$ is the Roe state related to $\boldsymbol{U}_i$ and $\boldsymbol{U}_j$ defined as:

$$\bar{\mathbf{U}}_{ij}^n = h^* \begin{pmatrix} 1 \\ u^* n_x + v^* n_y \\ v^* n_x - u^* n_y \\ C^* \\ \frac{Z_i + Z_j}{2h^*} \end{pmatrix}, \quad \text{such as:} \quad \begin{cases} h^* = \frac{h_i + h_j}{2} \\ u^* = \frac{u_i\sqrt{h_i} + u_j\sqrt{h_j}}{\sqrt{h_i} + \sqrt{h_j}} \\ v^* = \frac{v_i\sqrt{h_i} + v_j\sqrt{h_j}}{\sqrt{h_i} + \sqrt{h_j}} \\ C^* = \frac{C_i\sqrt{h_i} + C_j\sqrt{h_j}}{\sqrt{h_i} + \sqrt{h_j}} \end{cases}$$

The sign matrix of the Jacobian matrix is defined by: $sgn[\nabla \mathbf{F}_\eta(\bar{\mathbf{U}})] = \mathcal{P}(\bar{\mathbf{U}}) sgn[\mathcal{D}(\bar{\mathbf{U}})] \mathcal{P}^{-1}(\bar{\mathbf{U}})$, where $\mathcal{P}(\bar{\mathbf{U}})$ and $\mathcal{P}^{-1}(\bar{\mathbf{U}})$ are the eigenvector and eigenvalue matrices respectively. These matrices are defined as follows:

$$sgn[\mathcal{D}(\bar{\mathbf{U}})] = \begin{pmatrix} sgn(\bar{\lambda}_1) & 0 & 0 & 0 & 0 \\ 0 & sgn(\bar{\lambda}_2) & 0 & 0 & 0 \\ 0 & 0 & sgn(\bar{\lambda}_3) & 0 & 0 \\ 0 & 0 & 0 & sgn(\bar{\lambda}_4) & 0 \\ 0 & 0 & 0 & 0 & sgn(\bar{\lambda}_5) \end{pmatrix}, \quad \text{with:} \quad \begin{cases} \lambda_1 = u_\eta - \sqrt{gh} \\ \lambda_2 = 0; \quad sgn(\bar{\lambda}_2) = 0 \\ \lambda_3 = \lambda_4 = u_\eta \\ \lambda_5 = u_\eta + \sqrt{gh} \end{cases}$$

$$\mathcal{P}(\bar{\mathbf{U}}) = \begin{pmatrix} 1 & 1 & 0 & 0 & 1 \\ u_\eta^* - \sqrt{gh^*} & 0 & 0 & 0 & u_\eta^* + \sqrt{gh^*} \\ u_\tau^* & u_\tau^* & 1 & 0 & u_\tau^* \\ C^* & C^* & 0 & 1 & C^* \\ 0 & \frac{(u_\eta^*)^2 - gh^*}{gh^*} & 0 & 0 & 0 \end{pmatrix}, \quad \mathcal{P}^{-1}(\bar{\mathbf{U}}) = \begin{pmatrix} \frac{u_\eta^* + \sqrt{gh^*}}{2\sqrt{(gh^*)}} & -\frac{1}{2\sqrt{(gh^*)}} & 0 & 0 & \frac{\sqrt{(gh^*)}}{2(\sqrt{(gh^*)} - u_\eta^*)} \\ 0 & 0 & 0 & 0 & \frac{gh^*}{(u_\eta^*)^2 - gh^*} \\ -u_\tau^* & 0 & 1 & 0 & 0 \\ -C^* & 0 & 0 & 1 & 0 \\ \frac{\sqrt{gh^*} - u_\eta^*}{2\sqrt{(gh^*)}} & \frac{1}{2\sqrt{(gh^*)}} & 0 & 0 & \frac{\sqrt{(gh^*)}}{2(\sqrt{(gh^*)} + u_\eta^*)} \end{pmatrix}.$$

Once the projected state $\mathbf{U}_{ij}^n$ is calculated, the quantity W_{ij}^n will be calculated using the following transformations:

$hu^n{}_{ij} = (hu_\eta)^n{}_{ij} n_x - (hu_\tau)^n{}_{ij} n_y$, and $hv^n{}_{ij} = (hu_\tau)^n{}_{ij} n_x + (hu_\eta)^n{}_{ij} n_y$. There for, the corrector stage is written using the states of the following mine:

$$\frac{dW_i}{dt} = -\frac{1}{|T_i|} \sum_{j \in N(i)} |\gamma_{ij}| \mathbb{F}(W_{ij}, \mathbf{n}_{ij}) + S_i \tag{7}$$

Where $\mathbb{F}(W_{ij}, \mathbf{n}_{ij}) := \mathbb{F}(W_{ij}) \cdot \mathbf{n}_{ij}$ is the physical flux applied to the state W_{ij} obtained in the predictor step.

Temporal discretization

The equation (7) will be solved with various temporal numerical schemes either implicit or explicit, amongst which the Euler, Rung-Kutta and Adams-Bashforth schemes etc. Here we have chosen the explicit Euler scheme, which has fairly and it is very simple and fast. The time domain is divided into N sub-intervals $[t_n, t_{n+1}]$ with time step $\Delta t = t_{n+1} - t_n$ for $n = 0,1,....,N$. W^n is the value of a generic function W at time t_n. The fully-discrete formulation of the equation (7) is given by:

$$W_i^{n+1} = W_i^n - \frac{\Delta t}{|T_i|} \sum_{j \in N(i)} |\gamma_{ij}| \mathbb{F}(W_{ij}^n, \mathbf{n}_{ij}) + \Delta t S_i^n \tag{8}$$

The above algorithm is well known and has with an explicit advection step a first order temporal accuracy for the system variables (4). In the next subsection, we will discuss the discretization of the bottom profile taking into account the equilibrium issue of the lake at rest (see e.g. [6, 8, 10]).

Bottom profile discretization

The treatment of source terms in shallow water equations is a challenge in many numerical methods (see [6, 12, 15]). In [4], an approximation of the source term S ni was proposed in the predictor stage. This approximation satisfies the exact conservation property also called "C-property", but the spatial accuracy was affected when simulating flows over domains with very irregular topography. In this study, we will use a modification of this approach that was published by EL Mahi et al. [3] on which the formulation of the source term to obtain an equilibrium scheme preserving the quiescent state while keeping the accuracy in space has been proved. We recall that a numerical scheme is said to verify the C-property, if applied to stationary the scheme finds.

$$h_i^n + Z_i^n = CONST \quad \text{and} \quad u_i^n = v_i^n = 0$$

Considering the system (4) for a stationary regime, the predictor step (6) is written we recall that a numerical scheme is said to verify the C-property, if applied to a stationary the scheme finds.

$$\begin{pmatrix} h_{ij}^n \\ 0 \\ 0 \\ (hC)_{ij}^n \end{pmatrix} = \begin{pmatrix} \frac{h_i^n + h_j^n}{2} \\ 0 \\ 0 \\ \frac{h_i^n C_i^n + h_i^n C_i^n}{2} \end{pmatrix}$$

Therefore, for a stationary flow, the corrective step is written.

$$\sum_{j \in N(i)} \begin{pmatrix} 0 \\ \frac{1}{2} g (h_{ij})^2 (n_{ij})_x |\gamma_{ij}| \\ \frac{1}{2} g (h_{ij})^2 (n_{ij})_y |\gamma_{ij}| \end{pmatrix} = \begin{pmatrix} 0 \\ -g \int_{T_i} h \partial_x Z dV \\ -g \int_{T_i} h \partial_y Z dV \end{pmatrix} \tag{9}$$

To approximate the source term in (9), the control volume T_i is first subdivided into three sub-triangles, as shown in Figure 2 below.

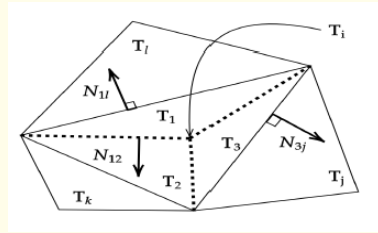

Figure 2: Generic definition of the Ω domain and the control cells of the mesh.

We use the following notations and expressions:

- $N_{xij} = (n_{ij})_x |\gamma_{ij}|$, and $N_{yij} = (n_{ij})_y |\gamma_{ij}|$,
- $\sum_{j \in N(1)} N_{x1j} = 0.$

Figure 2: Generic definition of the Ω domain and the control cells of the mesh. The source term can then be broken down as follows.

$$\int_{T_i} h \partial_x Z dV = h_1 \int_{T_1} \partial_x Z dV + h_2 \int_{T_2} \partial_x Z dV + h_3 \int_{T_3} \partial_x Z dV, \tag{10}$$

With h_1, h_2 and h_3 are the average values of h over T_1, T_2 and T_3 respectively.

Using the Gauss divergence formula for these three integrals and the fact that the stationary flow condition condition is also verified on each of the sub-triangles of T_i, the source term is written:

$$\int_{T_i} h \partial_x Z dV = -\frac{1}{2} \left(h_1 h_l N_{x1l} + h_2 h_k N_{x2k} + h_3 h_j N_{x3j} \right). \tag{11}$$

This reconstruction allows the corrective step (9) to be rewritten as two linear equations in h_1, h_2 and h_3.

$$\begin{aligned} \sum_{j \in N(i)} (h_{ij}^n)^2 N_{xij} &= h_1 h_l N_{x1l} + h_2 h_k N_{x2k} + h_3 h_j N_{x3j}, \\ \sum_{j \in N(i)} (h_{ij}^n)^2 N_{yij} &= h_1 h_l N_{y1l} + h_2 h_k N_{y2k} + h_3 h_j N_{y3j}. \end{aligned} \tag{12}$$

Which are completed by the following conservation equation:

$$h_1 + h_2 + h_3 = 3h_i \tag{13}$$

Once the mean values h_1, h_2 and h_3 are obtained, the background values Z_1, Z_2 and Z_3 on the sub-triangles are reconstructed in such a way that

$$Z_i + h_i^n = Z_j + h_j^n$$

Finally, the source term is approximated by.

$$\int_{T_i} h\partial_x Z dV = \frac{h_1}{2}(Z_l N_{x1l} + Z_2 N_{x12} + Z_3 N_{x13}) + \frac{h_2}{2}(Z_k N_{x2k} + Z_1 N_{x21} + Z_3 N_{x23}) + \frac{h_3}{2}(Z_j N_{x3j} + Z_1 N_{x31} + Z_2 N_{x32}) \tag{14}$$

With this new formulation of the source term, an equilibrium scheme is obtained which preserves the positivity of the water level and the concentration of the pollutant.

Treatment of friction terms

The friction terms are discretized using a fractional semi-implicit scheme [16]. For example, to evaluate the momentum, system (2) is decomposed into two equations.

$$\begin{cases} \dfrac{\partial h\mathbf{u}}{\partial t} = -\eta^2 g h^{-1/3}|\mathbf{u}|\mathbf{u} \\ \dfrac{\partial h\mathbf{u}}{\partial t} + \Phi_{h\mathbf{u}}(W) = -gh\nabla Z, \end{cases} \tag{15}$$

Where η is the Manning's coefficient and Φ_{hu} encompasses the convection and diffusion terms in the equation of motion in the x-direction, corresponds to the integral surface in equation (2) and is approximated as the sum over all edges of the control volume. In a first step, a linearized semi-implicit method is used to integrate the first equation of the system (15). In the second step, the value $(\tilde{hu})_i$ in (16) is taken as the initial condition for solving the second equation (15).

$$(\tilde{hu})_i = \frac{(hu)_i^n}{1 + \Delta t \eta^2 (h_i^n)^{-3/4}|\mathbf{u}|} \tag{16}$$

The same procedure is applied to the wind friction terms and the Coriolis terms.

Diffusion operator discretization

To complete the construction of the digital plan, the part concerning the diffusion. It is assumed here that the diffusion coefficients in the concentration equation are constant, so we have to evaluate the terms of the form.

$$\int_{T_{ij}} (hD_x\partial_x C \cdot n_x + hD_y\partial_y C \cdot n_y) d\sigma \tag{17}$$

The discretization of these diffusion flows on unstructured meshes is still a difficult problem. Many theoretical investigations and mathematical analyses have been directed towards this path. In this section, we present a finite volume scheme for this type of problem, when unstructured meshes are used. The algorithm is based on a Green-Gauss interpolation to construct the gradients at the mesh interfaces. The weak consistency of this scheme has been proven under a certain condition regarding the points of the interpolation. We write.

$$\int_{\gamma_{ij}} hD_x\partial_x \cdot n_x d\sigma = D_x h_{|_{\gamma_{ij}}} \partial_x C_{|_{\gamma_{ij}}} \int_{\gamma_{ij}} n_x d\sigma \tag{18}$$

The problem now depends on how to assess $\partial_x C$ on the γ_{ij}.

We construct the co-volume SRNL centered on the interface γ_{ij}, connecting the barycentres *L* and *R* of the two triangles having in

common the edge γ_{ij} and the two points *N* and *S* of the edge γ_{ij} (see the Figure 3). One can assume that the gradient is constant on the co-volume *SRNL*. According to Green-Gauss theorem the approximation leads to.

$$\nabla C_{ij} = \frac{1}{2\mu_{SRNL}} \left\{ (C_S - C_N)\vec{n_{LR}}|\gamma_{LR}| + (C_R - C_L)\vec{n_{ij}}|\gamma_{ij}| \right\}, \quad (19)$$

Where C_N, C_S, C_R and C_L represent respectively the values of the quantity *u* in the point *N, S, R* and L. $\vec{n}_{LR}$ is a unit normal vector of the co-volume face γ_{LR} and $|\gamma_{LR}|$ is its length. The others co-volume interfaces and their normal vectors are labeled analogically. μ_{SRNL} is the area of the co-volume *SRNL*.

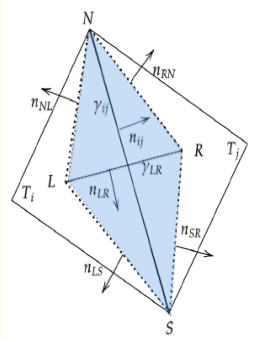

Figure 3: co-volume with Diamond shape.

The data at the *L* and *R* centres are known exactly, whereas the data at the *N* and *S* nodes must be determined by an interpolation procedure. For a node *P* in the mesh, a linear approximation of *C* is used over the set of cells containing the node of the triangle (see the Appendix of [13]).

Numerical Tests

To the best of our knowledge, the results to be presented here are obtained for the first time. All simulations presented in this section are performed with a time step *Δt* adjusted at each step according to the following expression:

$$\Delta t = CFL \cdot \min\left(\min_{\gamma_{ij}} \left(\frac{|T_i| + |T_j|}{2\gamma_{ij} \max_p |(\lambda)_{ij}^p|} \right), \min_{T_i} \frac{|T_i|}{2\gamma_{ij} \max(D_x, D_y)} \right)$$

λ_{ij}^p is the eigenvalue calculated at the interface γ_{ij} between the two cells T_i and *Tj*, and *CFL* is the current number set to 0.8 for all the test cases we will present here to ensure the stability of the stability of the numerical scheme.

Simulation of pollutant transport in the Nador lagoon

We propose here a test of the pollutant advection-diffusion equation in the Nador-Morocco lagoon. This test can model the contamination by the city's wastewater and consists to inject a pollutant from five source (Figure 6 left). Figure 4 shows the mesh (15244 elements and 7859 nodes) of the calculation domain, and Figure 5 shows the lagoon bathymetry. The mesh and the bathymetry were reconstructed from a point cloud recovered from a topographic map. The bottom of the lagoon is very irregular and has different scales in space, which can cause difficulties in the numerical plan. A special treatment, as shown in the numerical diagram, must therefore be considered for the source term.

In the initial state, the flow is assumed to be at rest with a zero concentration of the pollutant in the domain. At *t = 0s*, a pollutant is discharged during 1 hour from the five sources with a constant concentration *C* = 1 and a uniform velocity. The diffusion coeffi-

cients in the x and y directions are taken as constant $D_x = D_y = 0.001m^2/s$ and the Manning number $\eta = 0.02s/m^{1/3}$.

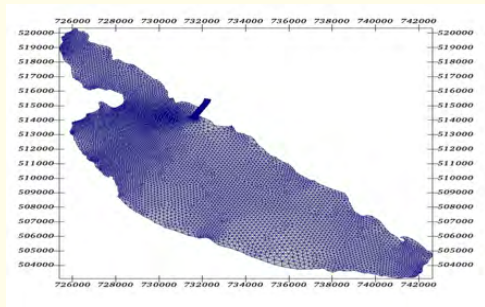

Figure 4: Non-uniform triangular mesh of the Nador lagoon.

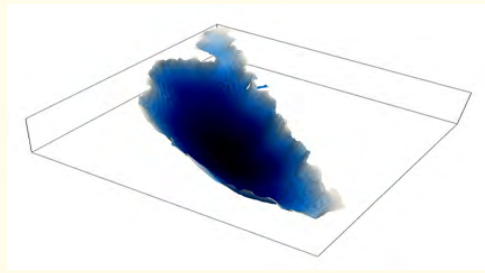

Figure 5: The bathymetry of the Nador lagoon.

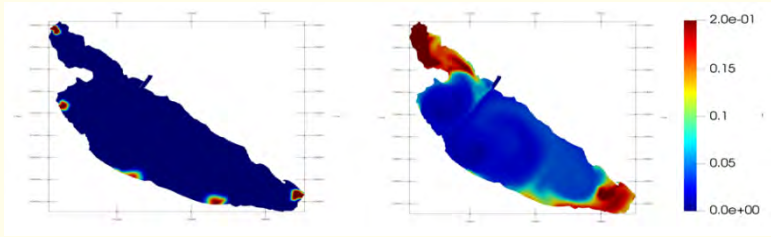

Figure 6: Pollutant sources (left), dispersion after 10 days (right).

Figure 6 right shows the evolution of pollutant concentration after 10 days. The pollutants coming from the five sources are mixed and form some vortices inside the lagoon, and go into the left and right corners because of less velocity in those sides. On these figures, one can note a good behavior on the numerical solution, but confirm the observations done by the Head of Public wastewater for the city of of the Nador City. This simulation is done using Manapy 2, and takes 1 hour to simulate 10 days using 32 MPI processors.

Conclusion

A coupled shallow water flow and advection-diffusion equation model was used to simulate the transport of pollutants in the Nador lagoon. To solve the model, we implemented a finite volume method using non-uniform triangular meshes. The method is simple, robust, and can be implemented for a large species transport system in a flow field driven by water flows. The method captures the

correct pollution dynamics and shows its ability to resolve pollution events in the lagoon.

Pollution events in the Nador lagoon under extreme hydraulic and wind regimes. We noticed that the results of our study are in good agreement with what happens in reality so we can say that we have a simulation that can predict the different situations resulting from this type of flow. An in-depth study is underway to take additional information into consideration; eg. The wind effects, tides information, etc..., to be closer to reality, and compute the residence time that takes the pollutant to be evacuated at the Mediterranean ocean.

References

1. E Audusse and M-O Bristeau. "A well-balanced positivity preserving "second-order" scheme for shallow water flows on unstructured meshes". Journal of Computational physics 206.1 (2005): 311-333.
2. F Benkhaldoun., et al. "A non-homogeneous riemann solver for shallow water equations in porous media". Applicable Analysis 95.10 (2016): 2181-2202.
3. F. Benkhaldoun., et al. "A new finite volume method for flux-gradient and source-term balancing in shallow water equations". Computer Methods in Applied Mechanics and Engineering 199.49-52 (2010): 3324-3335.
4. F Benkhaldoun., et al. "Well-balanced finite volume schemes for pollutant transport by shallow water equations on unstructured meshes". Journal of computational physics 226.1 (2007): 180-203.
5. F Benkhaldoun and L Quivy. "A non homogeneous riemann solver for shallow water and two phase flows". Flow, Turbulence and Combustion 76.4 (2006): 391-402.
6. A Bermúdez., et al. "Upwind schemes for the two-dimensional shallow water equations with variable depth using unstructured meshes". Computer methods in applied mechanics and engineering 155.1-2 (1998): 49-72.
7. A Bermudez and ME Vazquez. "Upwind methods for hyperbolic conservation laws with source terms". Computers & Fluids 23.8 (1994): 1049-1071.
8. EM Chaabelasri., et al. "Well balanced adaptive simulation of pollutant transport by shallow water flows: Application to the bay of tangier". International Journal of Hydraulic Engineering 3.1 (2014): 10-23.
9. S Ferrari and F Saleri. "A new two-dimensional shallow water model including pressure effects and slow varying bottom topography". ESAIM: Mathematical Modelling and Numerical Analysis-Modélisation Mathématique et Analyse Numérique 38.2 (2004): 211-234.
10. US Fjordholm., et al. "Well-balanced and energy stable schemes for the shallow water equations with discontinuous topography". Journal of Computational Physics 230.14 (2011): 5587-5609.
11. J-F Gerbeau and B Perthame. "Derivation of viscous saint-venant system for laminar shallow water numerical validation". 1.1 (2001): 89-102.
12. JM Greenberg and A-Y LeRoux. "A well-balanced scheme for the numerical processing of source terms in hyperbolic equations". SIAM Journal on Numerical Analysis 33.1 (1996): 1-16.
13. J Karel. "Numerical simulation of streamer propagation on unstructured dynamically adapted grids". PhD thesis, Université Paris-Nord-Paris XIII (2014).
14. J Kou., et al. "An energy stable linear numerical method for thermodynamically consistent modeling of two-phase incompressible flow in porous media". Journal of Computational Physics (2021): 110854.
15. M Lukacova-Medvidova. "Numerical modeling of shallow flows including bottom topography and friction effects". Proceedings of ALGORITMY (2005): 73-82.
16. L Monthe., et al. "Positivity preserving finite volume roe: schemes for transport-diffusion equations". Computer Methods in Applied Mechanics and Engineering 178.3-4 (1999): 215-232.
17. S Sahmim. "Un schéma aux volumes finis avec matrice signe pour les systemes non homogenes". PhD thesis (2005).
18. S Sahmim., et al. "A finite volume solver based on matrix sign for non homogeneous systems". Finite Volumes for Complex Applications IV (2005): 471-482.

19. S Sahmim., et al. "A sign matrix based scheme for non-homogeneous pde's with an analysis of the convergence stagnation phenomenon". Journal of Computational Physics 226.2 (2007):1753-1783.
20. Z Wang., et al. "A new fifth-order finite difference well-balanced multi-resolution weno scheme for solving shallow water equations". Computers & Mathematics with Applications 80.5 (2020):1387-1404.
21. M Ziggaf., et al. "The FVC scheme on unstructured meshes for the two-dimensional shallow water equations". International Conference on Finite Volumes for Complex Applications (2020): 455-465.

Volume 2 Issue 1 January 2022